Phase diagrams of polymer-dispersed liquid crystal systems of itraconazole – component immiscibility induced by molecular anisotropy

Agnieszka Kozyra[1], *Naila A. Mugheirbi*[1,2], *Krzysztof J. Paluch*[3], *Grzegorz Garbacz*[4], *Lidia Tajber*[1]*

[1]School of Pharmacy and Pharmaceutical Sciences, Trinity College Dublin, Dublin 2, Ireland.

[2]Drug Product Science and Technology, Bristol-Myers Squibb, East Brunswick, New Jersey, 08901, USA.

[3]School of Pharmacy and Medical Sciences, Faculty of Life Sciences, Centre for Pharmaceutical Engineering Science, University of Bradford, Richmond Road, Bradford, W. Yorks., BD7 1DP, UK.

[4]Physiolution GmbH, Walther-Rathenau Strasse 49a, 17489 Greifswald, Germany.

*To whom correspondence should be addressed: lidia.tajber@tcd.ie

Phone: 00353 1 896 2787

Keywords: itraconazole, nematic, smectic, phase diagram, miscibility, Flory-Huggins theory, Maier-Saupe-McMillan theory

Abstract

Liquid crystalline (LC) materials and their non-medical applications have been known for decades, especially in the production of displays, however the pharmaceutical implications of the LC state are inadequately appreciated and experimental data misunderstood leading to possible errors, especially in relation to physical stability of medicines. The aim of this work was to study LC phases of itraconazole (ITZ), an azole antifungal active molecule, and, for the first time, to generate full thermodynamic phase diagrams for ITZ/polymer systems taking into account isotropic and anisotropic phases that this drug can form. It was found that supercooled ITZ does not form an amorphous, but a vitrified smectic (vSm) phase with a glass transition temperature of 59.35 °C (determined using a 10°C/min heating rate), as evident from X-ray diffraction and thermomicroscopic (PLM) experiments. Two endothermic LC events with the onset temperature values for a smectic to nematic transition of 73.2±0.4 °C and a nematic to isotropic transformation at 90.4±0.35 °C and enthalpies of transition of 416±34 J/mol and 842±10 J/mol, respectively, were recorded. For the binary supercooled mixtures, PLM and differential scanning calorimetry showed a phase separation with birefringent vSm persistent over a wide polymer range, as noticed especially for the hypromellose acetate succinate (HAS) systems. Both, smectic and nematic, phases were detected for the supercooled ITZ/HAS and ITZ/methacrylic acid - ethyl acrylate copolymer (EUD) mixtures, while geometric restrictions inhibited the smectic formation in the ITZ/polyacrylic acid (CAR) systems. The Flory-Huggins lattice theory coupled with the Maier-Saupe-McMillan approach to model anisotropic ordering of molecules was successfully utilised to create phase diagrams for all ITZ/polymer mixtures. It was concluded that in a supercooled ITR/polymer mix, if ITZ is present in a liquid crystalline phase, immiscibility as a result of molecule anisotropy is afforded. This study shows that the LC nature of ITZ cannot be disregarded when designing stable formulations containing this molecule.

1. Introduction

Poor solubility and dissolution of many active pharmaceutical ingredients (APIs) has become an industry-wide concern. Approximately 40% of marketed APIs are classified as class II drugs with high permeability and low solubility, according to the Biopharmaceutics Classification System (BCS).[1] Conversion of crystalline APIs into dis(ordered), amorphous or liquid crystal (LC) forms is a route, which promises to greatly improve the solubility and consequently the oral bioavailability of these BCS class II drugs, as the solubility of disordered (translationally and/or orientationally) forms is likely to be several times higher than their crystalline counterparts.[2,3]

Amorphous materials have attracted major interest of pharmaceutical scientists and this attention is reflected in numerous publications presenting clear benefits of such materials, aimed mainly at improving bioavailability.[4] Amorphous solids are isotropic systems where the three-dimensional long-range order does not exist. They may exhibit a short-range molecular order and the molecules are conformationally flexible.[5] On the other hand, despite the general knowledge of LC phases for many materials, their applications, beside topical systems, have not been extensively recognised in the field of pharmaceutical materials. Liquid crystals can be defined as a state of matter in which the degree of molecular order is between that of a crystalline solid and an isotropic material. Therefore LCs, or mesophases, are also referred to as the fourth state of matter, as they possess mechanical, optical and structural properties between that of a three dimensionally ordered solid crystal and a completely disordered liquid or amorphous solid.[5] LC materials can be divided into two broad categories: thermotropic LCs and lyotropic LCs. Thermotropic mesophases are formed by heating a crystalline solid or by heating or cooling a mesogen.[5] When a mesophase appears on both heating and cooling it is termed enantiotropic. The mesophase that appears only on cooling of a material below its

melting point or heating a solid is termed monotropic.[6] On the other hand, lyotropic LCs are formed by dissolving an amphiphilic mesogen in a suitable solvent.

Disordered APIs have higher energy, entropy and free energy than the corresponding crystalline state.[7] This may lead to their enhanced solubility and bioavailability. However, it also creates the possibility of chemical degradation or spontaneous crystallisation upon storing or processing conditions.[8,9] LC phases are expected to be more chemically and physically stable than fully disordered, amorphous materials of the same composition.[4] Also, due to the higher Gibbs free energy in comparison to crystalline materials, the (apparent) solubility of mesophases is higher, as shown for fenofibrate calcium.[10]

Physical stability of disordered materials can be imparted by mixing them with polymers to form solid dispersions (SDs).[11] This approach is well known for fully disordered API molecules and if the drug and polymer are miscible and the drug loading is below the solubility equilibrium, the drug is molecularly dispersed in the polymer matrix and should form a thermodynamically stable, homogeneous solution without supersaturation and a risk of crystallisation.[12–14] LC phases are also able to form LC/polymer blends, in literature often referred to as polymer dispersed liquid crystals (PDLCs), and a wide range of non-pharmaceutical applications of PDLCs, such as electrooptical displays, shutters and membranes, have been investigated.[15] These materials, however, typically consist of LC droplets dispersed in a polymer matrix, thus are phase separated systems. As from the point of view of pharmaceutical applications homogenous dispersions are preferred, the phase behaviour of mesophases in binary mixtures is of utmost importance as it directly impacts the physical stability and performance of SDs. Thermodynamic phase diagrams have been recognised as a very beneficial tool in determining stability of binary polymer/API SDs, with the Flory-Huggins approach allowing miscibility/immiscibility of components to be determined.[12–14]

Itraconazole (ITZ) is an API from a group of triazole antifungal drugs used against various fungal species including *Cryptococcus, Candida, Aspergillus, Blastomyces* and *Histoplasma capsulatum var. capsulatum.*[16] ITZ is classified as a BCS II compound with extremely low aqueous solubility and poor dissolution rate. ITZ is a week base (pKa of ~3.7)[17] and its aqueous solubility is approximately 1 ng/ml at neutral pH and around 4 µg/ml at pH 1.[16] ITZ has a melting point of approximately 170 °C and a reported glass transition temperature of 59 °C.[18,19] The chemical structure of ITZ is shown in Figure 1. In addition to solubility issues, ITZ has the unusual ability to form a number of LC phases.[18,20,21] It forms two thermotropic LC phases, nematic and smectic A,[22,23] however a nematic, process-induced phase was also characterised for nanosized and spray dried ITZ as well as a 1:1 water:ITZ complex forming a smectic phase were recently isolated.[24]

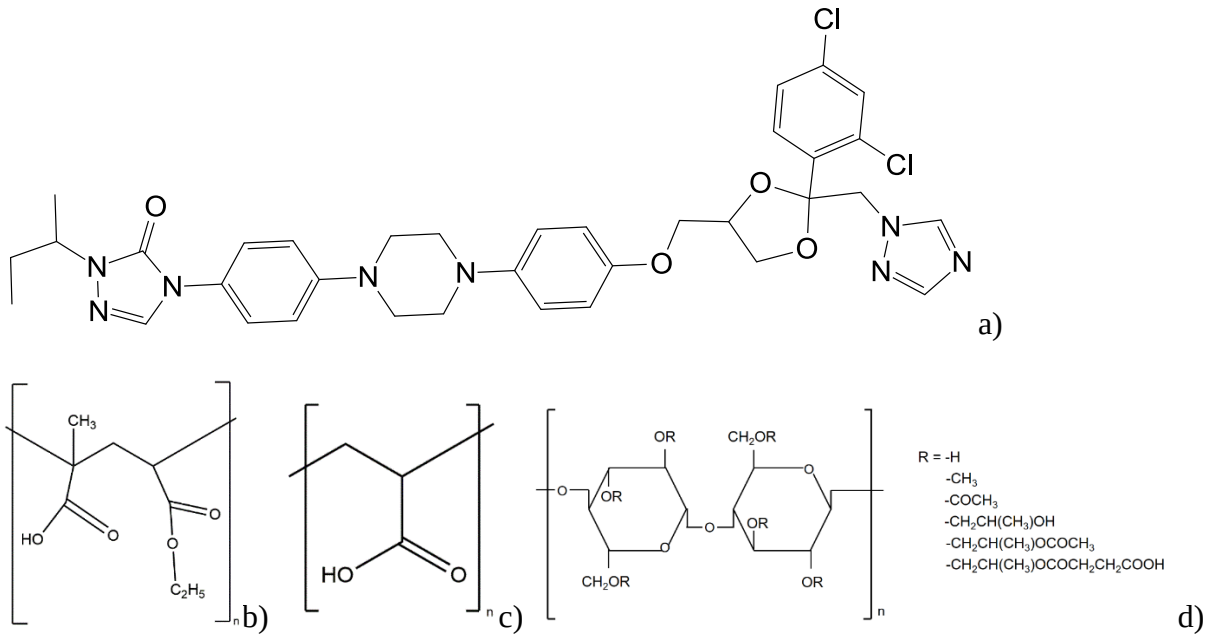

Figure 1. Chemical structure of: a) itraconazole (ITZ) and structures of monomers: b) Eudragit L100-55 (EUD), c) Carbopol 981 (CAR) and d) hypromellose acetate succinate (HPMCAS, HAS).[25]

Due to the very unfavourable biopharmaceutical properties of ITZ, many studies in relation to manufacturing its polymeric SDs have been published. Sarode et al. prepared X-ray

diffraction amorphous SDs of ITZ with hydrophilic polymers, including Eudragit EPO, Eudragit L-100-55, Eudragit L 100, HPMCAS-LF, HPMCAS-MF, Pharmacoat 603 and Kollidon VA-64.[26] The supersaturation levels of ITZ in non-sink conditions of simulated intestinal fluid (SIF) achieved with HPMCAS-LF, HPMCAS-MF and Eudragit L 100-55 were respectively 22, 19, and 7- times higher than the equilibrium solubility of ITZ in SIF.[26] Enteric polymers, including cellulose acetate phthalate (CAP) and polyvinyl acetate phthalate (PVAP), were selected by DiNunzio et al.[17] to produce amorphous SDs by ultra-rapid freezing. ITZ-CAP formulations demonstrated a significant improvement in the supersaturation level of ITZ in neutral media. This was due to the stabilising effect of the polymer and a 2-fold improvement in ITZ bioavailability in comparison to the currently marketed product (Sporanox®) was demonstrated.[17] Ternary amorphous SDs of ITZ in Eudragit L 100-55 containing either 20% or 40% Carbopol® 974P produced by hot melt extrusion were investigated by Miller et al.[27] The addition of 20% Carbopol® 974P very markedly extended the *in vitro* release of ITZ at 1 and 2 h after the acid-to-neutral pH change, respectively.[27]

The SDs produced in the above studies were all identified as being amorphous. However interestingly, Six et al.[20] and Janssens et al.[21,28] observed a phase separation of ITZ from Kollicoat IR® and Eudragit E100-based SDs. This phase separation was dependent on the API concentration and the drug phase identified as a "chiral nematic mesophase", but not as an amorphous solid. Kaminska et al. stated, based on thermal analysis, that octaacetylmaltose (a chemically modified disaccharide) was able to suppress the liquid crystalline ordering in ITZ in ITZ/octaacetylmaltose SDs.[29]

Considering the scarcity of data in relation to ITZ LC behaviour in polymeric SDs, the main aim of this study was to consolidate information on ITZ LCs, investigate the phase behaviour of ITZ when in binary mixtures with polymers and construct, for the first time, full phase diagrams for a pharmaceutical drug showing a liquid crystalline behaviour when mixed

with polymers. The Flory-Huggins theory for isotropic systems was coupled with the Maier-Saupe-McMillan approach for anisotropic mixing to support the construction of phase diagrams. Based on the previous reports, the following polymers presenting the benefits when incorporated in ITZ SDs and resulting in an improvement of the drug biopharmaceutical properties: Eudragit L100-55[26] (EUD), HPMCAS-MG[26] (HAS) and Carbopol[27] were selected.

2. Materials and methods

2.1. Materials

Itraconazole (ITZ) was donated by Welding GmbH (Hamburg, Germany). Methacrylic acid - ethyl acrylate copolymer (Eudragit L100-55, EUD) was kindly donated by Evonik Industries AG (Germany), polyacrylic acid (Carbopol 981, CAR) was purchased from BF Goodrich (USA), while hypromellose acetate succinate (Shin-Etsu AQOAT) grade MG (HPMCAS-MG, HAS) was donated by Shin-Etsu Chemical Co. Ltd. (Japan). Figure 1 shows structure of the API and polymers used, while Table 1 presents their physicochemical characteristics. HAS starting material was a coarse powder and it was comminuted at 400 rpm for 30 minutes with a planetary ball mill PM 100 (Retsch, Germany) at room temperature prior to mixing with ITZ. Ethanol (98%, analytical grade) used for content uniformity experiments was purchased from Cooley distillery.

Table 1. Physicochemical properties of ITZ, EUD, HAS and CAR. M_w - molecular weight, T_m^0 onset – onset temperature of melting, T_m^0 endset – endset temperature of melting, ΔH - heat of fusion, T_g – glass transition temperature and d - true density, N/A – not applicable.

Component	M_w (g/mol)	T_m^0 onset (°C)	T_m^0 endset (°C)	ΔH (J/g) and (J/mol)	T_g (°C)	d (g/cm^3)
ITZ	705.6	166.1±0.2	168.05±0.35	81.54±0.35 (57534±247)	59.35±0.35	1.4±0.0
EUD	320,000	N/A	N/A	N/A	114.4±0.25	1.3±0.0

HAS	18,000	N/A	N/A	N/A	117.3±0.2	1.3±0.0
CAR	1,250,000	N/A	N/A	N/A	129.4±0.3	1.5±0.0

2.2 Methods

2.2.1 Preparation of physical mixtures

All physical mixtures (in w/w ratios) of ITZ (crystalline, as supplied) and each of the polymers investigated (EUD, HAS or CAR) were prepared by ball milling at 400 rpm for 10 minutes, with a planetary ball mill PM 100 (Retsch, Germany) at room temperature. It was shown before that this procedure did not reduce crystallinity of the starting material (Figure SI.1).[14] The total amount of powder, 0.5 g, was loaded into the stainless steel milling container with a volume of 25 ml and two stainless steel balls (15 mm in diameter) were used. The collected samples were stored in a desiccator over silica gel at 5 ˚C until use.

2.2.2 Content uniformity determination

The content uniformity test was carried out on the 9:1 ITZ/polymer w/w physical mixtures after ball milling and this analysis was performed five times for each system. A UV spectrophotometric method was used on a double beam UV-visible spectrophotometer (model 1700Pharma, Shimadzu, Japan) with two matched quartz cells with a 1 cm light path. Ethanol was used as a solvent for all analyses. Absorbance of each solution against ethanol was recorded at 262 nm. Six point calibration curves were obtained for each of the ITZ/polymer systems with a correlation coefficient (R^2) of at least 0.998. The single results were found to be deviating by no more than ±1.5% from the desired 90% ITZ content and the average results were deviating by no more than ±1.1% from the 90% ITZ content.

2.2.3 Thermal analysis

2.2.3.1 Melting point depression measurements

The melting events of crystalline ITZ in the physical mixtures prepared as described in Section 2.2.1 were measured using a PerkinElmer Diamond DSC unit (Waltham, MA, USA) with HyperDSC. The unit was refrigerated using an ULSP B.V. 130 cooling system (Ede, Netherlands) and operated under a nitrogen flow of 40 ml/min. The gas flow was controlled using a PerkinElmer Thermal Analysis Gas Station (TAGS). The instrument was calibrated for melting temperature onset and enthalpy with indium. Before the measurement, the samples loaded in the DSC standard aluminium pans (5-8 mg) were first annealed in an oven (Memmert, Germany) at a temperature 10 °C above the glass transition temperature (T_g) of the polymer for 2 h. The annealing time was chosen to be 2 h based on comparison of the heat of fusion values obtained for the non-annealed and annealed for 2, 4, and 6 h 9:1 ITZ/polymer w/w physical mixtures. The heat fusion of samples annealed for 2, 4, and 6 h did not differ; therefore it was assumed that annealing time of 2 h would be sufficient. Samples were then cooled down to room temperature and the final sample weight was calculated.

The DSC programme used to determine the melting point depression due to the presence of the polymer was as follows: samples were first heated from 25 to 120 °C at a heating rate of 10 °C/min and then a heating rate of 1 °C/min was applied to obtain the melting temperature value as close to the equilibrium as possible.[14] All curves were evaluated and the values of melting onsets, melting endsets (offsets) and heat of fusions were calculated. All analyses were performed in duplicate for each sample.

2.2.3.2 Liquid crystalline (LC) phase transition measurements

LC phase transition events of ITZ and ITZ/polymer mixtures were determined using the Perkin Elmer Diamond DSC setup as described above. Samples (physical mixtures prepared as described in Section 2.2.1) weighing between 3-5 mg were first heated from 25 to 180 °C, cooled to 25 °C and then re-heated to 180 °C. A heating/cooling rate of 10 °C/min was used in all steps. All analyses were performed in duplicate for each sample.

2.2.3.3 Determination of glass transition temperatures (T_gs)

T_gs of ITZ/polymer mixtures were determined using the Perkin Elmer Diamond DSC setup as described above. Samples (physical mixtures prepared as described in Section 2.2.1) weighing between 5-8 mg were preheated in the DSC pans from 100 to 170 °C at a 10 °C/min heating rate, cooled to 30-40 °C below the expected T_g at a programmed cooling rate of 300 °C/min (flash cooling) and then a step scan (modulated temperature) method was applied to determine the T_g. For the step scan, the samples were heated to 30-40 °C above the expected T_g at 5 °C/min in 2 °C steps. A 1 min isothermal step was applied between each of the dynamic steps. All analyses were performed in duplicate for each sample.

2.2.3.4 Thermogravimetric analysis (TGA)

TGA of the polymers used for this study was performed using a Mettler TG 50 module linked to a Mettler MT5 balance (Mettler Toledo, Switzerland). Sample weights between 9-11 mg were used and placed into open aluminium pans. Measurements were performed from 25 to 200 °C at a 10 °C/min heating rate. Analysis was carried out in the furnace under nitrogen purge and monitored by Mettler Toledo STARe software (version 6.10). TGA analysis of polymers used in this study was carried out to ensure that the melting point measurements would not be affected by polymer decomposition. The weight loss due to thermal decomposition was 0.6±0.2, 2.3±0.7, 0.8±0.1 and 1.1±0.1% for ITZ, EUD, HAS and CAR when analysed up to 180 °C.

2.2.4 Powder X-ray diffraction (PXRD)

Powder X-ray diffraction measurements at room temperature (RT-PXRD) were performed on samples placed on a standard glass sample holder using a Rigaku Miniflex II desktop X-ray diffractometer (Rigaku, Japan) with a Haskris cooling unit (Grove Village, IL, USA). RT-PXRD patterns were recorded from 2 to 40 on the 2θ scale at a step of 0.05 /s. The

X-ray tube was operated under a voltage of 30 kV and current of 15 mA. Samples for RT-PXRD analysis first were melted in the oven at 180 °C on glass supports and cooled down to room temperature prior to the analysis.

Temperature controlled PXRD (VT-PXRD) was performed on an X'Pert-PRO (PANalytical, Netherlands) X-ray diffractometer equipped with an Anton Paar TTK-450 sample stage (Anton Paar, Austria). VT-PXRD patterns were collected from 5 to 40 2θ at a continuous scanning rate of 0.12 2θ/second. The X-ray tube was operated under a voltage of 40 kV and current of 40 mA.

2.2.5 Polarised Light and Hot Stage Microscopy (PLM)

PLM experiments were performed using an Olympus BX53 polarising optical microscope equipped with a U-POT cross polarizer, a Linkam hot stage and a Q IMAGING Fast 1394 camera (Olympus, Japan) at x500 magnification. The hot stage ramp, for thermomicroscopic investigations, was performed from 25 to 180 °C using a heating rate of 10 °C/min. Samples for PLM experiments were prepared by melting on a microscope glass slide at 170 and 180 °C in the oven (Memmert, Germany). When the powdered mixture was fully melted, a glass coverslip was placed on top, and the sample was allowed to cool at room temperature.

2.2.6 True density measurements

True density was measured by an AccuPyc 1330 Pycnometer Micromeritics™, using helium (99.995% purity) to determine the volume of the sample. A 1 cm^3 aluminium sample cup was used for all samples and was filled up to 2/3rd of its nominal volume. The instrument was calibrated immediately before the analysis. All analyses were performed in duplicate for each sample.

2.2.7 Mathematical modelling and statistical analysis

Modelling of phase diagrams and statistical analysis was performed in Origin 2018. Non-linear least squares curve fits to experimentally determined data were obtained by applying the Levenberg-Marquardt iteration algorithm until the Chi-square tolerance value of 1×10^{-9} was reached and the fit converged. No weighting for parameters was applied.

3. Results and discussion

3.1. Liquid crystalline properties of itraconazole

The ability of itraconazole (ITZ) to form liquid crystal phases was previously reported by Six and co-workers.[18] The authors stated that on reheating, the melted drug showed a glass transition temperature (T_g) at 59 °C and two endothermic reversible transitions at 74 and 90 °C. The peak at 90 °C was interpreted as the transition of the isotropic liquid into a chiral nematic mesophase, while the transition occurring at a lower temperature (at 74 °C) was assigned as being most likely due to rotational restriction of the molecules.[18] Further research on the molecular dynamics of ITZ by dielectric spectroscopy was later conducted by Tarnacka et al.[22] and Mapesa et al.[23] concluding that these endothermic transitions are in fact related to the formation of a nematic phase (LC_{N-I}), seen as an endothermal transition at 90 °C, and a smectic A phase (LC_{Sm-N}), represented as an endothermal transition at 74 °C, phase.

With the previously published literature in mind, in this work, a range of characterisation techniques were applied to characterise ITZ further. ITZ was subjected to a thermal analysis cycle consisting of a first heating to 170 °C (as the melting point of ITZ is 166 °C)[18], flash cooling to 25 °C and then re-heating at 10 °C/min. At higher temperatures crystallisation and melting processes were seen. A small endotherm at around 160 °C, preceding the main melting peak, was observed (Figure 2a). Recently, polymorphism of ITZ was described by Zhang et al.[30], however no sign of a polymorphic transition was observed for this sample under polarising light microscopy (Figure 2a) and by PXRD (Figure SI.2). Thus it

is likely that the origin of this low magnitude endotherm is the presence of small crystallising particles of ITZ with the melting point following a Gibbs-Thomson relationship, similarly as described previously for fenofibrate.[31]. The positions of the LC thermal transitions (Figure 2a) were in agreement with the data reported by Six et al.[18] Nevertheless, this group observed that the glassy ITZ prepared by cooling from its melt did not crystallise on heating and that crystallisation was mechanically induced by scratching.[18]

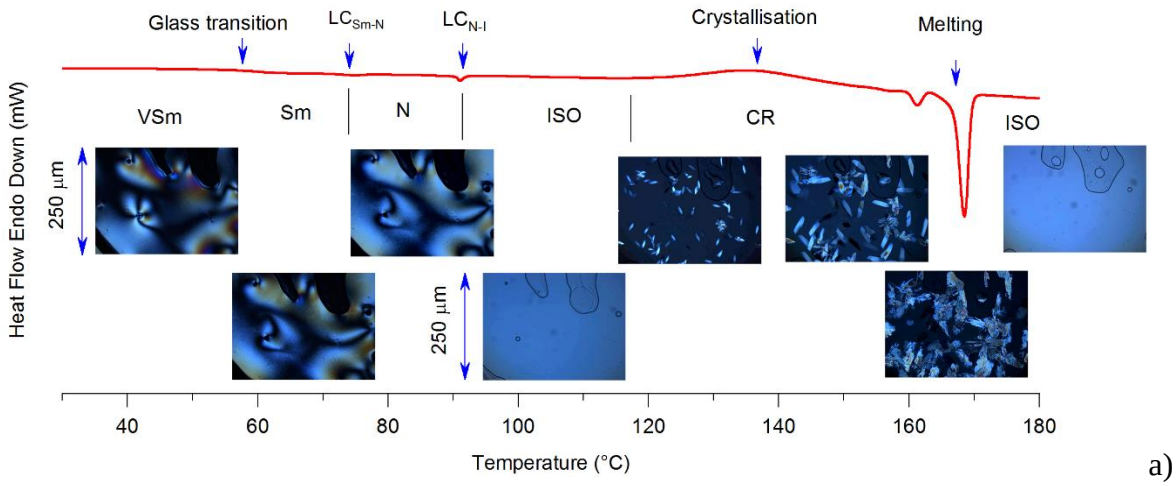

a)

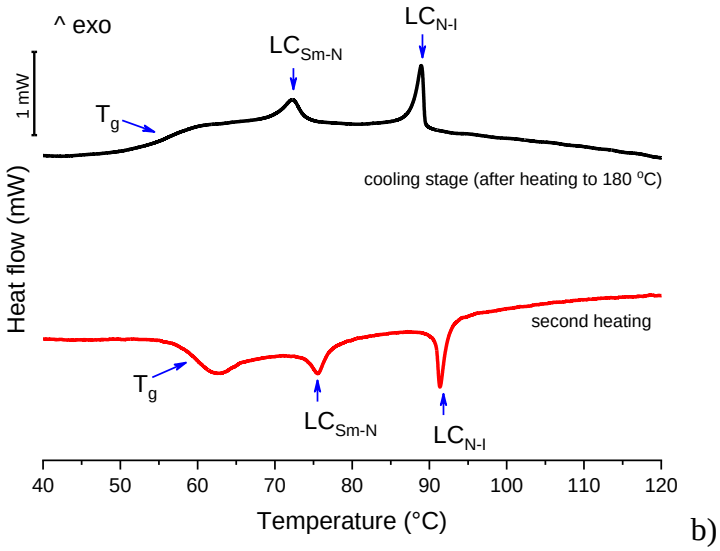

b)

Figure 2. a) DSC and thermomicroscopical analysis of second heating of ITZ, previously heated to 170 °C and cooled to 25 °C. The images present morphology of ITZ phases identified: VSm – vitrified smectic, Sm – smectic, N - nematic phase, ISO – isotropic phase, CR-crystallisation. b) DSC

thermograms of ITZ on cooling after heating to 180 °C (black solid line) and reheating the sample from its vitrified phase.

Thus, in another experiment the end temperature of the first heating stage was increased to 180 °C, followed by cooling to 25 °C (slow cooling at 10 °C/min) and reheating at the same rate. As shown in Figure 2b, the DSC trace on reheating (second heating) showed a T_g at 59.35±0.35 °C, followed by two endothermic LC transitions with the onset temperature values for the LC events of 73.2±0.4 °C (LC_{Sm-N}) and 90.4±0.35 °C (LC_{N-I}) with the enthalpies of transition of 416±34 J/mol and 842±10 J/mol, respectively. Thus, these values are typical of nematic and smectic transitions as tabulated by Sackmann.[32] No cold crystallisation on reheating was observed and the position and the heat of transition of the LC events was unaffected by the thermal treatment applied. It was also determined that a change in the cooling rate from 300 °C/min to 10 °C/min during the cooling step had no effect on the position and magnitude of the LC peaks. A consecutive heating/cooling treatment showed the reversibility of the LC transitions (Figure 2b) and the enantiotropic nature of both LC transitions. The most likely explanation for crystallisation of ITZ on the DSC run when the sample was first heated to 170 °C might be in the thermal lag of the sample (the melting point is only 166 °C) that resulted in some crystalline material still being present in the melted sample when the cooling stage began. Therefore, to avoid sample crystallisation, heating to 180 °C in the first stage was applied to all further investigations.

Polarising microscopy (PLM) is probably the most widely used technique to identify different LC phases as they appear to have distinct textures.[33] Based on the orientation of LC molecules one can distinguish between different phases. A sample of nematic or smectic C LC viewed by PLM often displays a colourful Schlieren texture. Between crossed polarisers, Schlieren textures show an irregular network of dark brushes, which correspond to the

extinction position of the nematic LC.[33] A smectic A phase viewed by PLM appears as a focal-conic fan texture. It develops directly from a nematic phase or isotropic liquid as batonnets grow, merge and eventually generate this characteristic texture.[33] The ITZ sample prepared by first heating the crystalline material to 180 °C and then cooling down to room temperature was clearly birefringent at 25 °C under PLM, showing a mixture of focal-conic fan and Schlieren textures along with spontaneously formed homeotropic fields (dark areas) (Figure 3a). Therefore, this material cannot be classified as an amorphous or a completely disordered phase. Several samples of vitrified ITZ were prepared proving reproducibility of the results (Figure 3a). For most of the samples colourful focal-conic fan textures as well as four-brush Schlieren textures were seen (Figure 3a) suggesting a material with a smectic (A or C) arrangement.

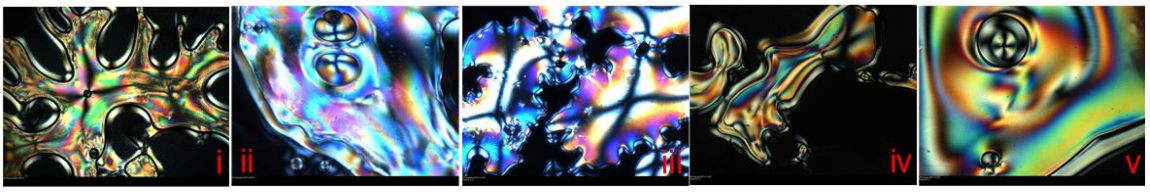

(a)

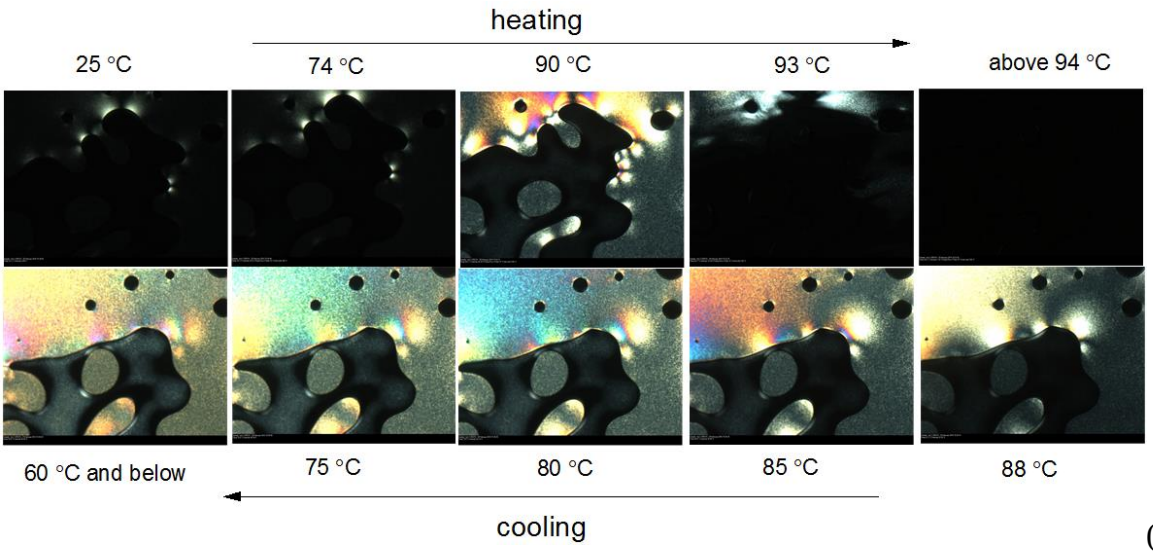

(b)

Figure 3. Textures of unaligned LC phases on untreated glass observed between crossed polarizers. (a) ITZ at 25 °C. The photo is of pure ITZ, which was first heated to 180 °C and then the melt cooled down to 25 °C. (b) PLM-HS analysis of ITZ. The ITZ sample was first heated to 180 °C and melt cooled down to 25 °C. The photos in the upper section indicate the re-heating stage (second heating), while those in the bottom section on cooling from re-heating.

Morphology of the vitrified ITZ sample subjected to a heating/cooling cycle of 25-100 °C at a rate of 10 °C/min is shown in the Figure 3b. On heating, a change was noticeable at about 74 °C. This corresponds to the first LC transition recorded in the DSC thermogram (Figure 2) at the same temperature. A growing increase in light intensity was visible up to 90 °C, where it reached its maximum intensity. This relates to another LC transition at around 90 °C, consistent with the DSC data. Above 90 °C, a gradual decrease in light intensity was noticed, reaching its minimum value at 93 °C. During the cooling stage, the first change was observed at about 88 °C. A growing increase in light intensity was visible cooling down to 60 °C, where it reached its maximum (Figure 3b).

RT-PXRD analysis performed on ITZ which was heated to 180 °C and then cooled down to room temperature showed two sharp peaks at 2θ of 2.97° (d-spacing 29.67 Å) and 5.96° (d-spacing 14.92 Å). There was also a major diffuse maximum at 2θ of 19° (Figure 4a). The peaks at around 3 and 19° 2θ corresponded well to the position of predicted maxima, normally located at $Q = 2\pi/l_o$ and $Q=2\pi/w_o$, where Q is the scattering wavevector and l_o and w, are the length and width of the molecule, respectively.[34] Molecular dimensions of ITZ were calculated from the crystal structure, CSD code: TEHZIP using Mercury 3.7 and the length and width of ITZ measured 28.05 Å and 5.42 Å, respectively. For a smectic phase the position and intensity of the diffraction peaks, typically sharp due the high degree of periodicity over large distances, are related to the long range organisation of the phase and in the ITZ sample shown

as the peak at app. 6° 2θ.[34] Thus the phase, resulting from heating ITZ past its melting point and cooled down to room temperature has a smectic arrangement, as suggested by PLM.

VT-PXRD was used to further investigate the LC phase transitions of ITZ (Figure 4b). The crystalline sample of ITZ was melted on the XRD sample holder at 180 °C. It was then cooled down to 25 °C followed by reheating to 100 °C at a heating rate of 10 °C/min. VT-PXRD spectra collected during cooling stage, showed a peak at 2θ of 5.88° (d-spacing 15.01 Å) beginning to appear at 60 °C. This sharp peak was persistent during further cooling down to 25 °C (Figure 4b). This clearly indicates a long range organisation of the LC phase and strongly suggests the smectic phase formation. Similarly, on reheating the same peak was evident, but this time reduction in peak intensity was noticed (Figure 4c).

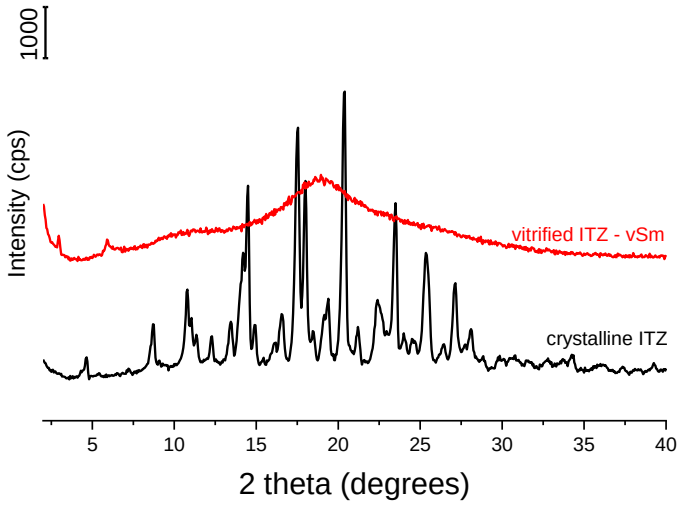

a)

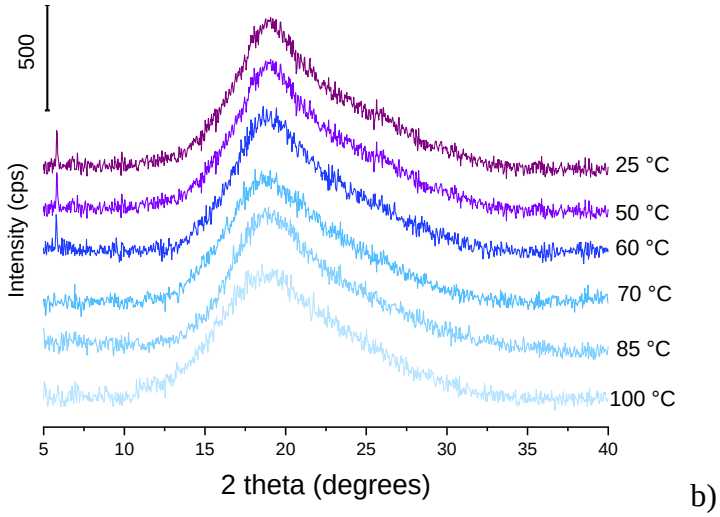

b)

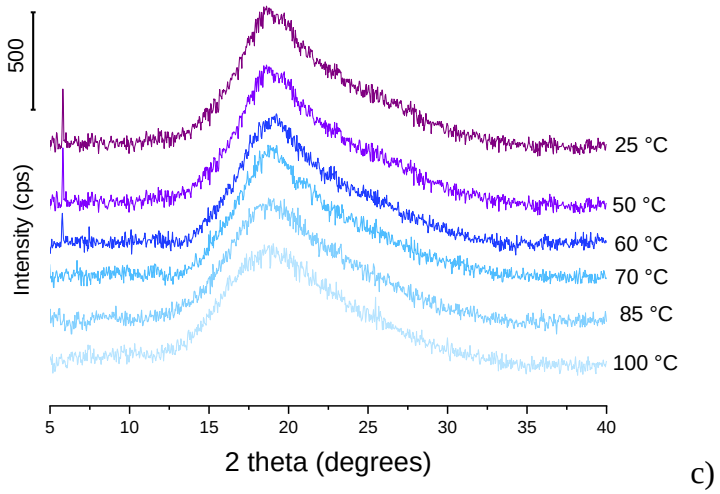

c)

Figure 4. a) RT-PXRD of crystalline and vitrified ITZ. b) VT-PXRD of ITZ on cooling. The sample was first heated to 180 °C. c) VT-PXRD of ITZ on second heating. The sample was first heated to 180 °C and cooled to 25 °C.

PLM-HS and PXRD studies clearly indicate that ITZ forms an ordered, anisotropic structure at 25 °C on cooling from its melt and that the molecular organisation of this phase is of a smectic and not a fully disordered, amorphous phase, as sometimes misinterpreted and referred to in many publications.[30,35,36] DSC thermogram, however, displays a T_g transition on cooling at 56 °C and therefore, consistent with the accepted nomenclature[37], this phase should be referred to as a vitrified smectic phase. It should be highlighted that the phenomenon of a

glass transition is not exclusive to amorphous materials. It has been long recognised that many other substances, even with a partly crystalline structure and with a long-range structural order (e.g. plastic crystals, liquid crystals, spin glasses etc.) may exhibit this transition.[38,39] Another interesting observation that can be made in relation to the T_g of ITZ (56 °C, 329 K) is that it can be considered as relatively high in comparison to its melting point (T_m) of 166 °C (439 K) with the T_g/T_m ratio of 0.75. This value falls within the range of 0.6-0.8 as reported by Kerc and Srcic[40], however it needs to be acknowledged that T_g values of nematic or smectic glasses (vitrified phases) are generally higher than those of fully disordered materials.[41]

3.2 Thermomicroscopic studies of ITZ/polymer systems

Observing the formation of a vitrified, glassy phase of ITZ on quench cooling, a frequent method used to obtain amorphous pharmaceuticals, an important question had arose: Is this phase formed when in a mixture with polymers? The production of polymeric solid dispersions (SDs) of ITZ, as a means of improving apparent solubility and dissolution rates thus enhancing bioavailability of the drug is well known and numerous accounts on this topic have been published.[17,26,27] However, when screening the available information, it becomes evident that only one research group has reported that a liquid crystal phase of ITZ may be present in such SDs.[20,21,28] A phase separation induced by anisotropy of an LC phase can be detrimental to the performance and long term stability of ITZ formulations, as discussed later.

A screening approach was adopted first, whereby 8:2 w/w ITZ/polymer mixtures were first prepared as described in Section 2.2.5 and then subjected to a heating/cooling treatment. Birefringence of the samples was clearly observed at 25 °C for the vitrified samples (Figure 5), regardless of the polymer (EUD, HAS or CAP) used.

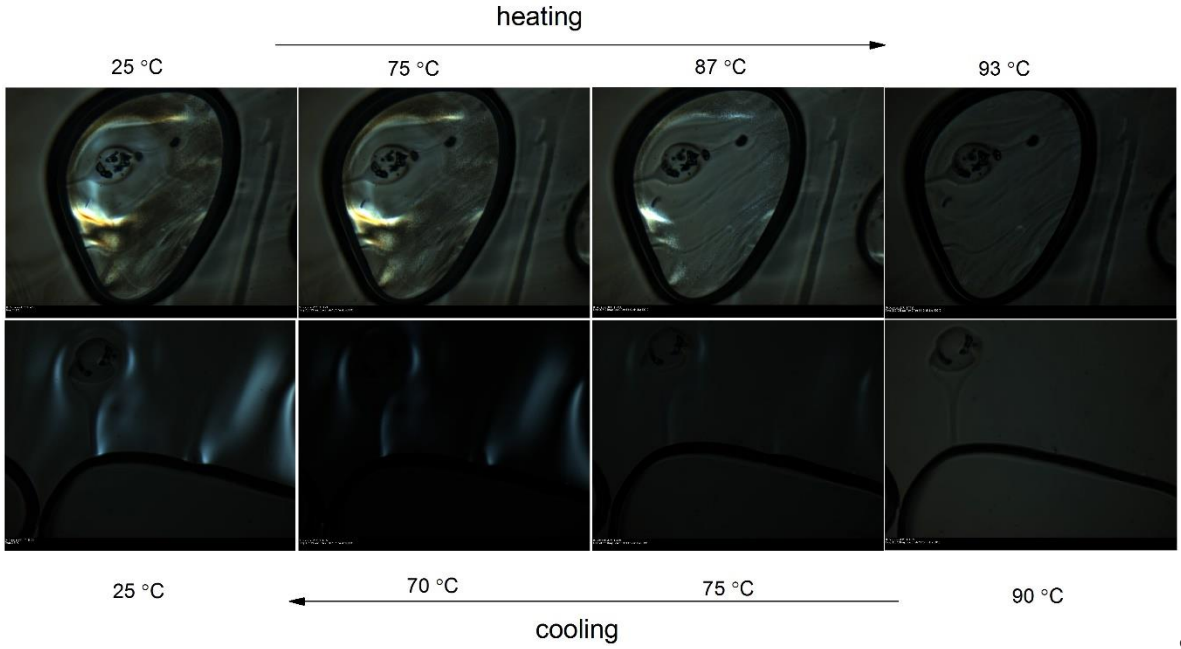
heating
25 °C
75 °C
87 °C
93 °C
25 °C
70 °C
75 °C
90 °C
cooling

a)

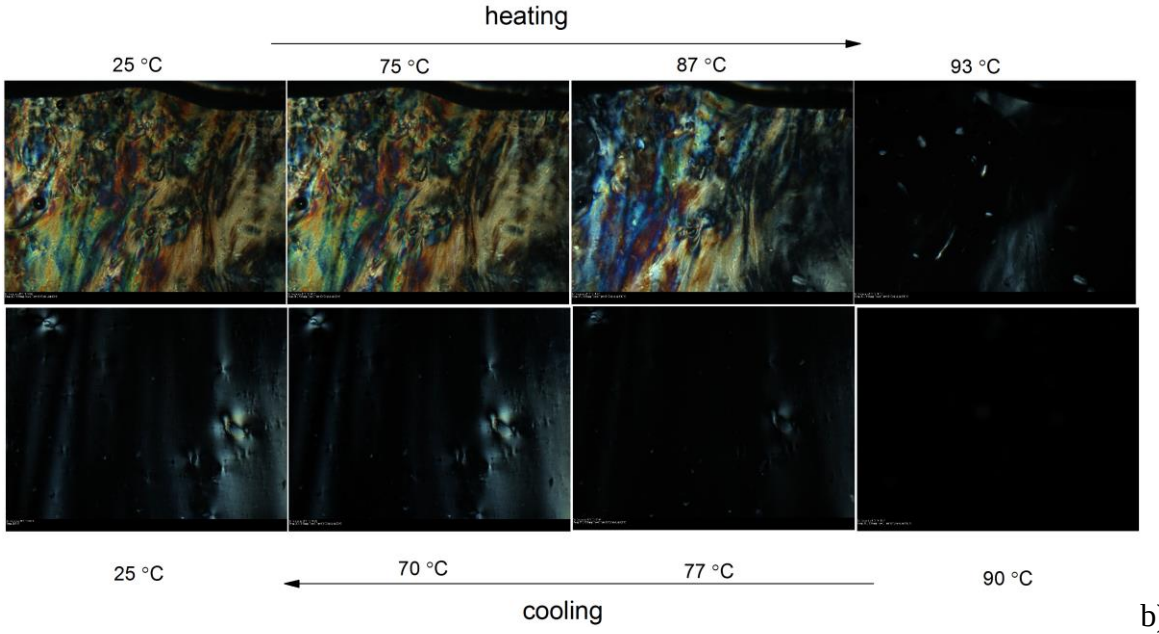
heating
25 °C
75 °C
87 °C
93 °C
25 °C
70 °C
77 °C
90 °C
cooling

b)

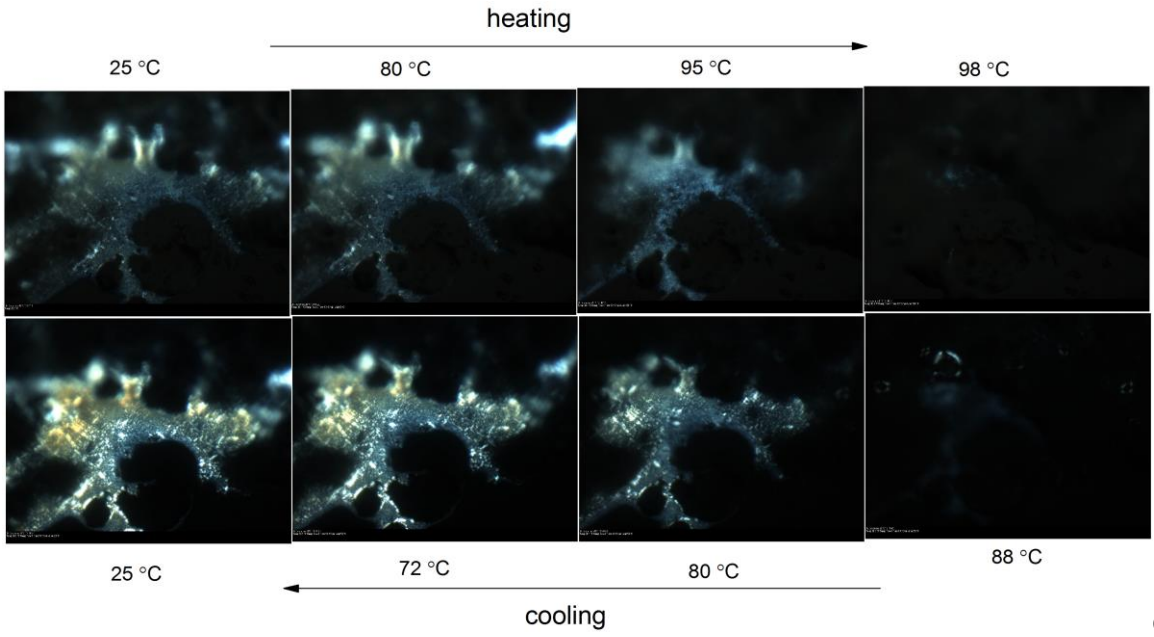

Figure 5. PLM-HS analysis of: a) 8:2 ITZ/EUD w/w, b) 8:2 ITZ/HAS w/w and c) 8:2 ITZ/CAR w/w. A heating/cooling cycle at a rate of 10 °C/min was used for all samples.

During the heating stage, the LC_{Sm-N} transition, expected at about 74-75 °C, was not seen by PLM in any of the analysed ITZ/polymer systems as no visible change was recorded regarding birefringence of these samples (Figure 5). In relation to the LC_{N-I} transition, expected to appear at around 90 °C, a clear change in the appearance of the ITZ/EUD and ITZ/HAS samples was recorded at 93 °C, while for the ITZ/CAR combination at 98 °C. Above 100 °C all samples remained isotropic and no birefringent regions were visible.

During the cooling stage, birefringent regions started to emerge only at 75 °C for ITZ/EUD and at 77 °C for ITZ/HAS samples (Figures 5a and 5b). No sign of the LC_{N-I} transition was apparent. The ITZ/CAR system showed a different behaviour as morphology of this sample changed at 88 °C with birefringent droplets forming at this temperature (Figure 5c). At 80 °C these droplets were fully formed and no further change in their birefringence upon cooling to 25 °C was seen (Figure 7). Inspecting closely the microscopic images it became obvious that the shape and position of the droplets remained almost the same during the heating/cooling cycle. Therefore this system appears to be more viscous (also consistent with

the high molecular weight of this polymer as presented in Table 1) in comparison to the ITZ/EUD or ITZ/HAS samples. The results also suggest that the ITZ/CAR system is more likely to form only one LC phase, most likely a nematic, rather than the more organised, smectic phase as ITZ molecules may have restricted movement due to the high viscosity of the polymer.

3.3 DSC analysis of liquid crystalline transitions for ITZ/polymer systems

DSC analysis of ITZ/EUD and ITZ/HAS systems revealed the presence of both, LC_{Sm-N} and LC_{N-I}, transitions for ITZ contents of at least 80% w/w. A decrease in the onset temperature values for the LC events was noticed in comparison to the values for pure ITZ (Figure 6a and b).

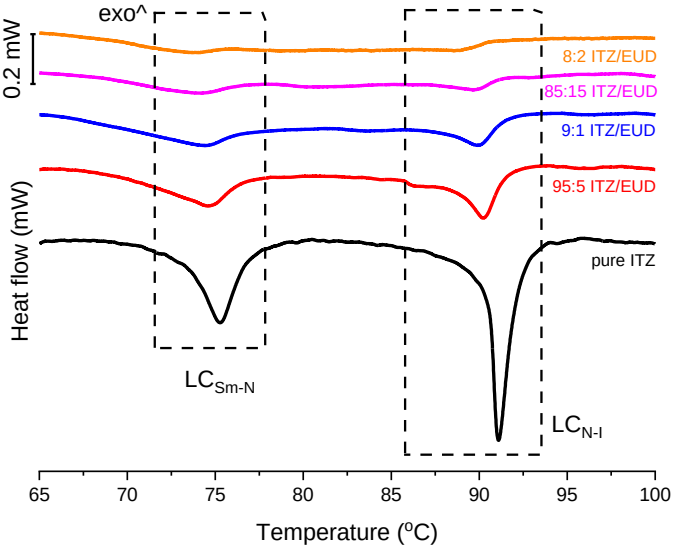

a)

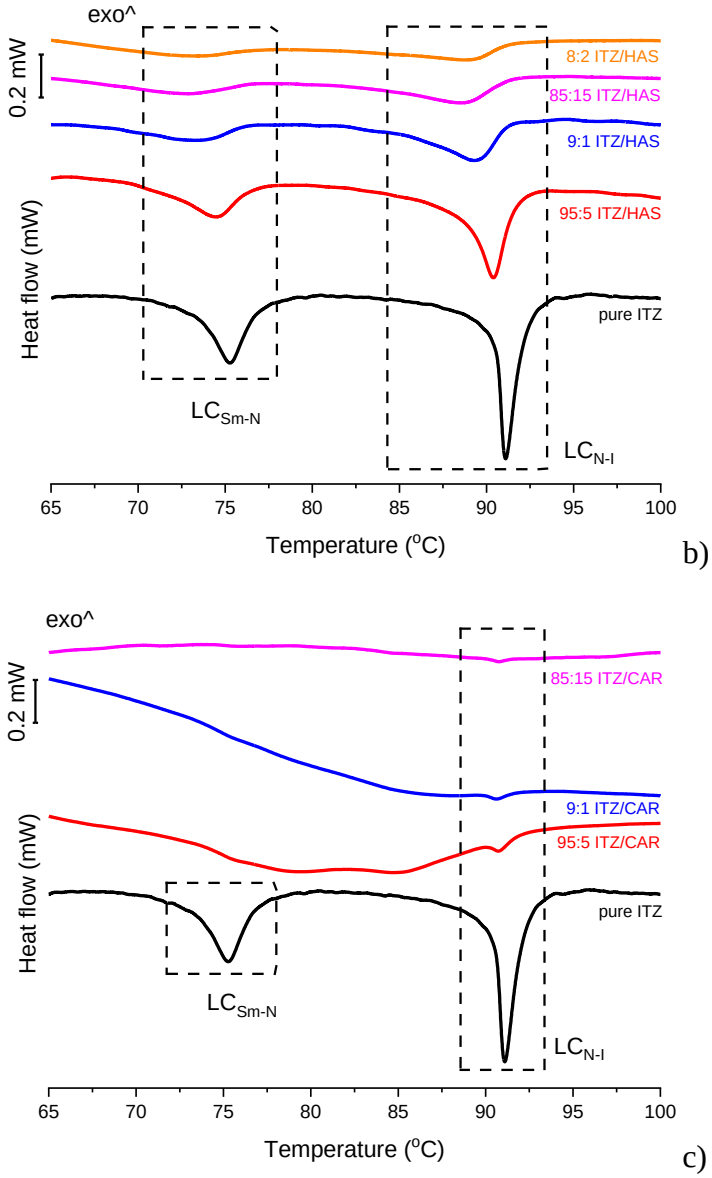

Figure 6. DSC thermograms of ITZ/polymer systems presenting the liquid crystalline transitions in ITZ. a) ITZ/EUD, b) ITZ/HAS and c) ITZ/CAR. The ITZ/polymer ratios are weight ratios; the temperature range for the LC transitions are marked by broken lines.

The largest decrease in the onset temperature for the LC transitions, in comparison to pure ITZ, was observed for the 8:2 ITZ/HAS w/w sample, with 66.65±0.1 and 82.1±0.5 °C recoded for LC_{Sm-N} and LC_{N-I}, respectively. For the EUD/ITZ combination the decrease in the onset temperature values was moderate, with the LC_{Sm-N} transition beginning at 70.0±0.1 °C and the LC_{N-I} transformation starting at 87.6±0.2 °C. This compares with 73.2±0.4 °C and

90.4±0.35 °C recoded for pure ITZ. Thus EUD and HAS are able to depress the onset temperature of LC transitions and work on the principles of miscible impurities. Interpreting these results in relation to ITZ miscibility, HAS is more likely to be miscible with ITZ than EUD. For the ITZ/CAR system only the LC_{N-I} transition was recorded by DSC and no significant difference was observed in relation to the onset temperature of this transition (Figure 6c).

Dispersions of ITZ/Eudragit E100 containing more than 13% of ITZ and produced by extrusion were identified by Six et al. as mixtures of molecular dispersions of the drug and polymer as well as liquid crystalline ITZ.[20] In fact, while the authors report the presence of only a "chiral nematic" phase, both LC transitions were clearly visible on the DSC thermogram shown in the report. Janssens and co-workers seen signs of a "glassy chiral nematic mesophase" of ITZ appearing at a drug load of 30% w/w for spray dried samples and at 22.5% w/w for the film casted systems. For the spray dried system only one LC endotherm was present, of the LC_{N-I} transformation, interpreted that ITZ was made to a disordered mesophase resulting from the interference of the polymer and the process.[21] Two LC transitions in samples composed of ITZ and Kollicoat IR® (a polyvinyl alcohol–polyethylene glycol copolymer) and processed by hot stage extrusion were recorded for the drug concentration 40% or higher.[28] In relation to the behaviour of investigated ITZ/CAR systems exhibiting only one LC transition, this could be caused by the strong polymer-polymer interactions[42] (though no evidence for intermolecular interactions was found in the present work by FTIR) and/or geometric inhibitions restricting the formation of a smectic phase, which is more ordered than a nematic and requires more space for the molecules to assembly.[43]

As evident from the DSC studies and data presented above, at least a part of ITZ was present in the drug/polymer mix as a liquid crystal. As numerous studies show, typically part of the LC remains separated (as evident from Figure 6) and some of the LC phase dissolves in

the polymer matrix to form a molecular dispersion.[15,44] The fraction of ITZ remaining in the LC phase can be quantified taking into consideration the enthalpy of a LC transition (Eqn. 1):

$$P(x) = \frac{\Delta H_{LC}(x)}{\Delta H_{LC}(LC)} \quad \text{(Eqn. 1)}$$

where x is the weight ratio of ITZ, P(x) is the ratio of the mass of phase-separated LC to the total mass of the blend and $\Delta H_{LC}(x)$ and $\Delta H_{LC}(LC)$ are the enthalpies (in J/g) for the LC transitions (LC_{Sm-N} and LC_{N-I}) for the blend and pure LC, respectively.[15] Relationships between P(x) and x for the various ITZ/polymer blends considering both LC transitions, LC_{Sm-N} and LC_{N-I}, separately are presented in Figure 7.

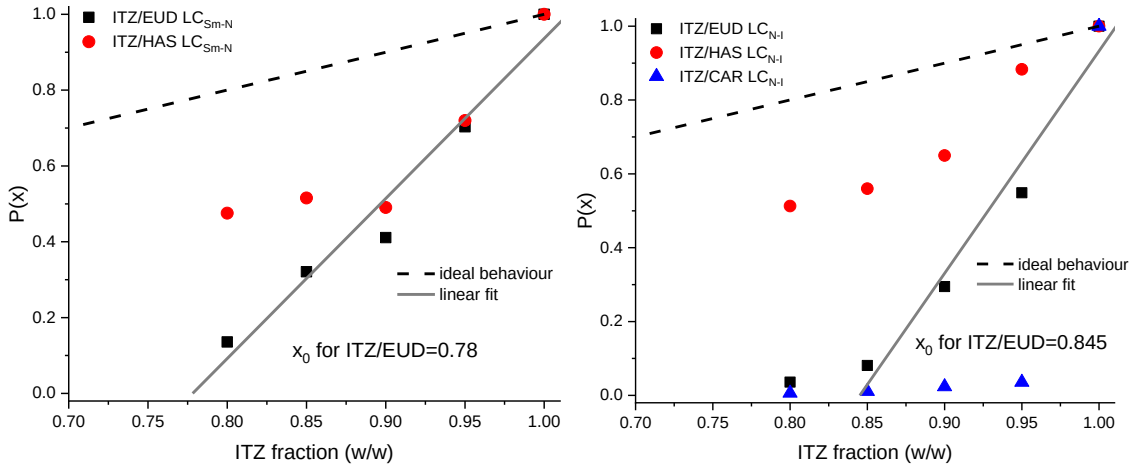

Figure 7. The mass ratio of phase separated ITZ as a liquid crystalline phase (P(x)) versus the total weight fraction of ITZ in the polymer blend. The dashed black line indicate the ideal P(x) versus ITZ weight fraction relationship if there was no solubility of ITZ in the polymer. The solid grey lines represent linear fits to ITZ/EUD data points, while x_0 is the ITZ weight fraction when P(x)=0, i.e. the drug concentration fully soluble in the polymer. Please note that the experimental data point for LC_{N-I} at x=0.8 was omitted in the linear fit for ITZ/EUD.

Some researchers have found that the P(x) versus x relationship can be linear[15,44], however this applies here to the ITZ/EUD system only with the drug solubility limits in the polymer determined for LC_{Sm-N} and LC_{N-I}, of 0.78 and 0.845 ITZ weight fraction, respectively.

Therefore, considering just the linear fits to the experimental points, the EUD content in those blends must be at least around 20% w/w to form a homogenous, non-separated blend. For the HAS systems, the LC phases of the drug were well persistent at concentrations much lower than 80% w/w ITZ and a non-linear relationship of P(x) versus x was observed. However, both LC_{Sm-N} and LC_{N-I} were seen to behave in a similar, non-linear manner. For the CAR/ITZ systems, a very abrupt decrease in the LC ITZ fraction was noted, as at 95% w/w ITZ only 3.6% of ITZ was separated from the blend. At 85% w/w ITZ the content of separated drug was only 1%.

3.4 Phase diagrams of ITZ/polymer systems

The phase behaviour of a low molecular weight drug substance and a polymer binary mixture in the isotropic state can be described by the Flory-Huggins (F-H) lattice theory, which is an extension of the concept of regular solutions on polymer solutions.[45] Over the last decade, this theory has been applied to describe and predict compatibility/miscibility of a number of API/polymer systems.[13,46–50] Readers are referred to those papers in relation to finding out more details. However, the F-H theory alone cannot be used to describe the phase behaviour of a binary composition made of a liquid crystalline compound with a polymer due to the inherent anisotropy of LC phases. Thus an extended approach to the F-H theory needs to be employed with the total Gibbs free energy of such a system (f) represented as the combination of two constituents, the free energy ($f^{(i)}$) of mixing of isotropic liquids, as described by the F-H lattice theory, and the free energy ($f^{(a)}$) due to anisotropic ordering of molecules.[44,51–53]

The F-H free energy ($f^{(i)}$) of mixing of isotropic liquids can be described by Eqn. 2[51,54]:

$$\frac{\Delta f^{(i)}}{RT} = \phi ln\phi + \frac{1-\phi}{m}\ln(1-\phi) + \chi\phi(1-\phi) \quad \text{(Eqn. 2)}$$

Where T is temperature (in K), R is the gas constant (in $J \cdot mol^{-1} \cdot K^{-1}$), ϕ is the volume fraction of the API (ITZ), m is the volume ratio of the polymer to drug volume and χ is the F-H

interaction parameter. The interaction parameter χ characterises the difference in interaction energies in the mixture, therefore two situations are possible. One, if there is a net attraction between molecules of different kinds, then $\chi < 0$ and a single phase mixture should be favoured for all compositions. However, if there is a net repulsion between molecules of different kinds then $\chi > 0$ and phase separation is most likely to occur in this case. To summarise, a necessary condition of miscibility is that the free energy of mixing is negative, therefore χ has to be negative or slightly positive.[55]

The free energy ($f^{(a)}$) due to anisotropic ordering of molecules for the nematic and/or smectic arrangement is described by the Maier-Saupe-McMillan (M-S-M) theory[44,56]:

$$\frac{\Delta f^{(a)}}{RT} = \phi\left[\frac{1}{2}\,v(S^2 + \xi\sigma^2)\phi - lnZ\right] \text{ (Eqn. 3)}$$

where ν is the temperature-dependent ($v=4.54T_{I\_N}/T$, where T_{I_N} is the isotroptic-nematic transition temperature (in K)) parameter describing interactions between the molecules in the nematic phase and S is the nematic order parameter, where $S=0.5(3\langle\cos^2\theta\rangle-1)$ with θ being the angle between a reference axis and the director of the liquid crystalline molecule, ξ is a smectic interaction parameter, σ is a smectic order parameter and Z is the partition function in the smectic order.

In relation to fitting the ITZ solid-isotropic (liquid) transition in the polymer systems, the parameter χ was calculated using the melting point depression method based on the F-H theory[12,50] using the following equation (Eqn. 4):

$$\left(\frac{\mathbf{1}}{T_m} - \frac{\mathbf{1}}{T_m^{\boldsymbol{o}}}\right) = \frac{-RT}{\Delta H_{fus}}\left[ln\boldsymbol{\phi} + \left(\mathbf{1} - \frac{\mathbf{1}}{\boldsymbol{m}}\right)(\mathbf{1} - \boldsymbol{\phi}) + \boldsymbol{\chi}(\mathbf{1} - \boldsymbol{\phi})^{\mathbf{2}}\right] \qquad \text{(Eqn. 4)}$$

where T_m and T_m^0 are the melting points (in K) of the drug in the binary mixture and pure drug, respectively, ΔH_{fus} is the heat of fusion of the pure drug (in $kJ\cdot mol^{-1}$). The parameter m can be calculated as per Eqn. 5, where M_w is the molecular weight and d is the true density (in $g\cdot cm^{-3}$):

$$m = \frac{M_{w\,(poly)}}{d_{poly}} \Big/ \frac{M_{w\,(drug)}}{d_{drug}} \qquad \text{(Eqn. 5)}$$

The phase diagrams presented in Figure 8 were constructed using the values presented in Table 1 and the data points were obtained in the following manner. Firstly, the solid-isotropic (liquid) line was constructed using the heating rate of 1 °C/min to provide sufficient time to achieve the melting temperature values as close to the solubility equilibrium as possible (Section 2.2.3.1). It was previously documented that both the heating rate and the annealing time have an impact on the melting point measurements.[49,57] Secondly, the T_g values were determined by heating ITZ/polymer physical mixtures past the melting point of ITZ and flash cooled to prevent, as far as possible, molecular ordering upon cooling. A modulated DSC programme was then used to determine the experimental T_g midpoints (Section 2.2.3.3). Thirdly and finally, LC transitions were measured on samples melted past the melting point of ITZ, cooled to 25 °C at a rate of 10 °C/min and re-heated at 10 °C/min, thus applying a "standard" thermal treatment (Section 2.2.3.2).

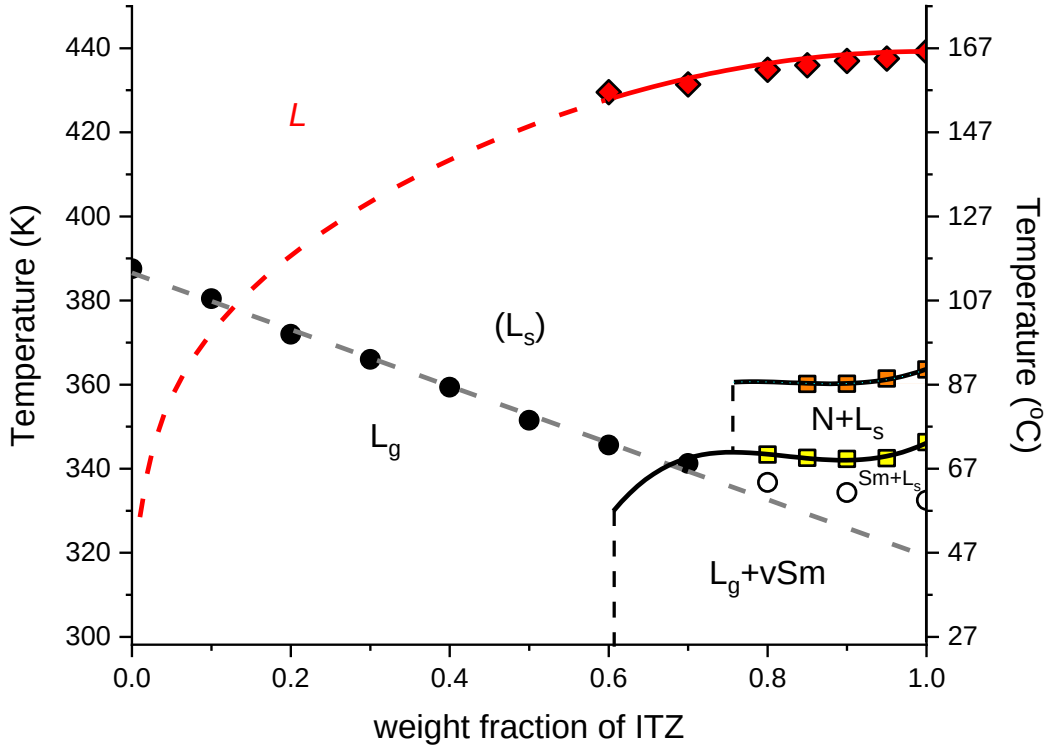

a)

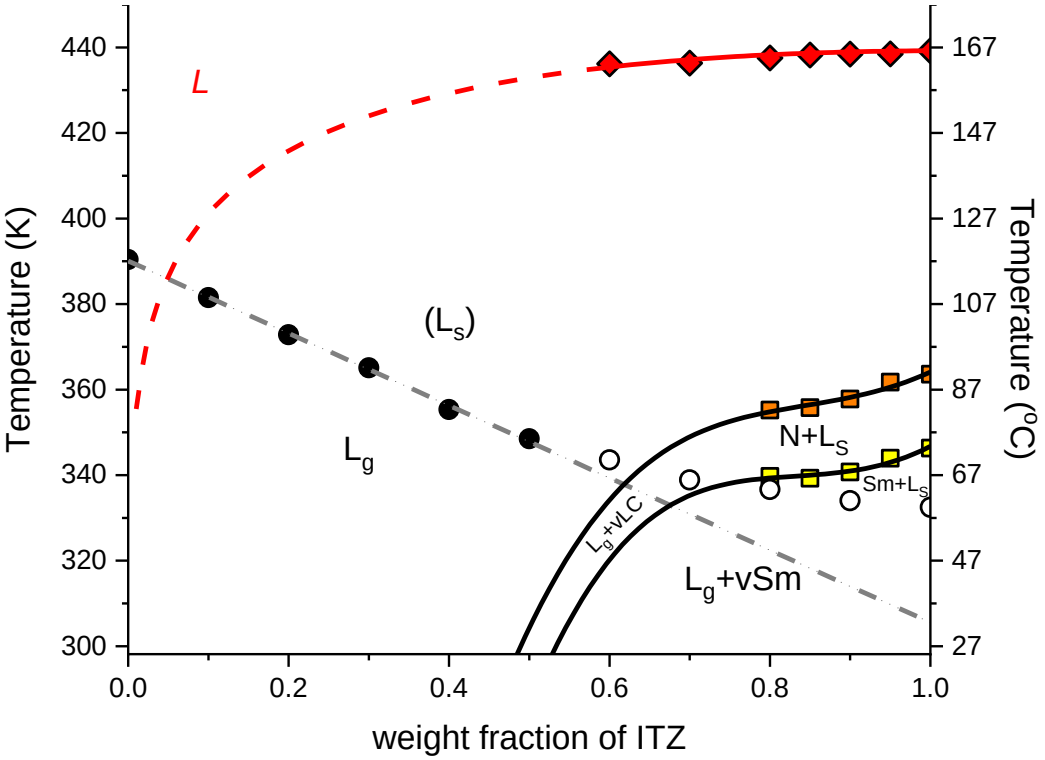
L
(L_S)
L_g
N+L_S
Sm+L_S
L_g+vLC
L_g+vSm
Temperature (K)
Temperature (°C)
weight fraction of ITZ
440
420
400
380
360
340
320
300
167
147
127
107
87
67
47
27
0.0
0.2
0.4
0.6
0.8
1.0

b)

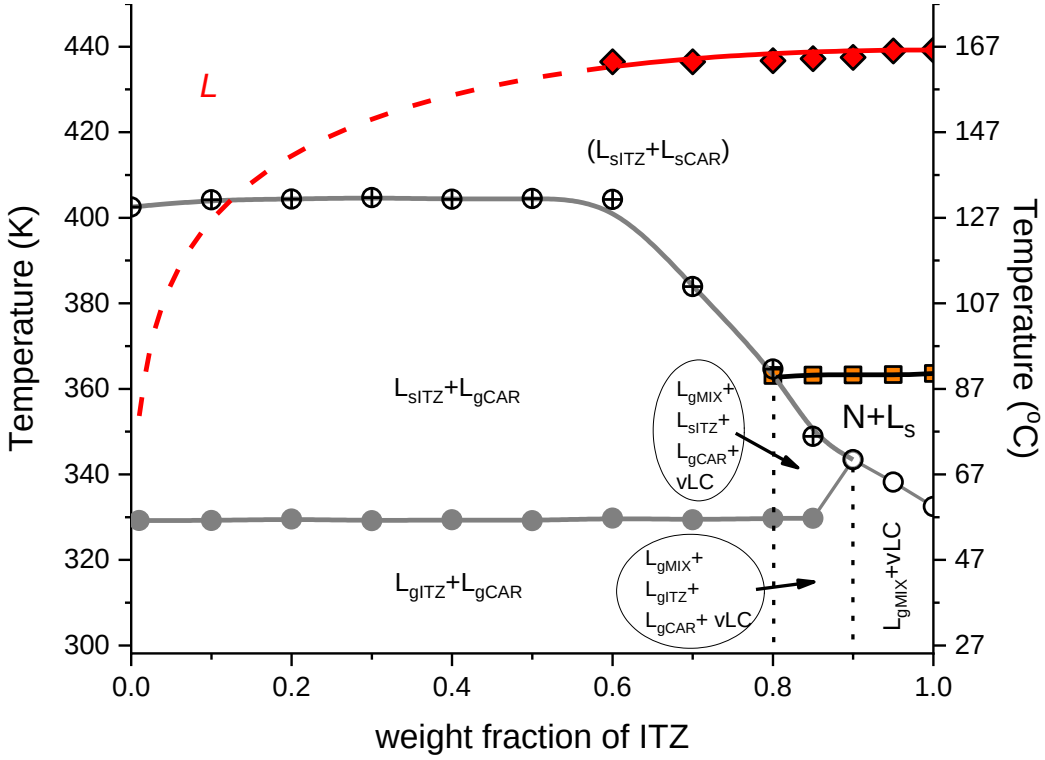
L
(L_sITZ+L_sCAR)
L_sITZ+L_gCAR
L_gMIX+ L_sITZ+ L_gCAR+ vLC
N+L_S
L_gITZ+L_gCAR
L_gMIX+ L_gITZ+ L_gCAR+ vLC
L_gMIX+vLC
Temperature (K)
Temperature (°C)
weight fraction of ITZ
440
420
400
380
360
340
320
300
167
147
127
107
87
67
47
27
0.0
0.2
0.4
0.6
0.8
1.0

c)

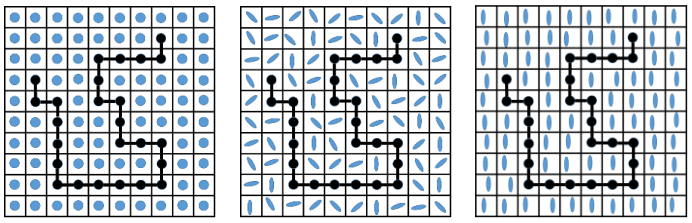
d)

Figure 8 Phase diagrams of the ITZ/polymer systems: a) ITZ/EUD, b) ITZ/HAS and c) ITZ/CAR. Symbols used: L – liquid, L_g – glass phase (below T_g), L_S – supercooled phase (above T_g), N – nematic, Sm – smectic, vSm – vitrified smectic, vLC – vitrified liquid crystal phase (uncertain identification), ITZ – Itraconazole, CAR – Carbopol and MIX – binary ITZ and CAR mixture. Broken grey lines through the T_g points (circles) for the ITZ/EUD and ITZ/HAS systems are linear fits; the fitted lines are based only on the T_g values for binary compositions with no apparent LC phases (black filled circles). Solid grey lines through the T_g points (circles) for the ITZ/CAR are for visual guide only. Grey filled circles represent experimental T_g of ITZ, open circles are T_gs of binary phases where LC phases were found, while crossed circles are T_gs of binary phases where polymer separation was found. Red lines are solid-isotropic (liquid) lines generated by fitting experimental points (diamonds) to the F-H theory, black lines are fitted LC lines (smectic–nematic and nematic-isotropic) to the experimental data (squares) using the F-H and M-S-M theories, while the broken lines indicate prediction beyond the experimental range. d) Schematic representation of polymeric ITZ dispersions with ITZ molecules in isotropic (left), anisotropic nematic considering an orientation order parameter (middle) and anisotropic smectic considering a one dimensional translational order parameter (right) arrangements.

3.4.1 Solid-isotropic (liquid) line

The solid-isotropic lines presented in Figure 8 were constructed based on the onset temperature of the ITZ melting peak, however there are differing opinions as to whether the onset[12,58] or endset (offset)[13,48,49] temperature of the melting endotherm of the drug better describes the miscibility of the API in the polymer. Thus, in order to compare and provide full information on ITZ miscibility in polymers in this study, both, the onset and endset temperature values for the drug were evaluated. It can be said that the solid-isotropic lines in Figure 8

represent the best case scenario of two component miscibility, determined on the ability of the melting point of crystalline ITZ to be depressed by the polymer presence.

Reliable DSC results providing data points for generation of forming the solid-isotropic lines were obtained only for the systems containing up to 40% w/w polymer. When comparing the data for the onset temperature of the melting event, there was an evident depression of the melting point in comparison with pure ITZ. The onset temperature of melting of pure crystalline ITZ, 166.1±0.2 °C, decreased with an increase in the polymer content as shown in Figure 8. For instance, at 60% w/w ITZ content, the largest reduction in the onset temperature was observed for the EUD sample, by approximately 3 degrees (163.1±0.2 °C). Smaller decreases, to 163.85±0.2 and 163.3±0.3 °C were recorded for the HAS and CAR samples, respectively. Therefore, considering the melting point depression results, EUD is more likely to be miscible with ITZ than HAS or CAR. No significant difference was observed in relation to the endset values of melting points. The variation in the endset of melting for all systems and at all compositions analysed was not more than ±0.5 °C from the temperature determined for pure, crystalline ITZ. Table 2 summarises the values of the interaction parameter (χ) calculated based on Eqns. 2 and 3.

Table 2. Values of the interaction parameter χ for the various ITZ/polymer systems estimated using the H-F theory (solid-isotropic lines) and a combination of F-H and M-S-M theories (LC lines).

System	Based on crystalline ITZ (solid-isotropic line)		Based on LC ITZ (smectic-nematic line)	Based on LC ITZ – (nematic-isotropic line)
	Onset points	Endset points		
ITZ/EUD	-1.65±0.28	0.71±0.05	0.715±0.02	0.70±0.01
ITZ/HAS	-0.03±0.12	0.65±0.04	0.72±0.04	0.69±0.065
ITZ/CAR	-0.27±0.26	0.67±0.02	N/A	0.59±0.01

As explained above, the sign of χ indicates whether the components in the binary system are miscible or not. For a system with $\chi<0$ a single phase mixture should be favourable for all

compositions (miscible system), while for χ>0, the phase separation is most likely to occur (immiscible system). From the endset points of the melting results, only positive values of χ were obtained. This suggests that ITZ and each of the polymers analysed should not be miscible. When the onset temperature values of the melting events were used, the values of χ were generally negative, however considering the standard deviation values (Table 2) some of them were only marginally negative, meaning that the components might not be fully miscible and may not form completely molecularly dispersed systems. The most negative value of χ was calculated for the ITZ/EUD system (Table 2).

The temperature and/or compositional dependence of the interaction parameter χ was also investigated, as if such dependence can be determined, it would allow extrapolation of the solid-isotropic line beyond the experimental points, thus be able to predict stability of a miscible blend and determine spinodal and binodal regions of the phase diagram.[48,54] A number of mathematical models were employed, described in details elsewhere[55,59,60], using the following equations:

$$\chi(T) = A + \frac{B}{T} \quad \text{(Eqn. 6)}$$

where A and B are constants related to entropic and enthalpy contributions, respectively.[55]

$$\chi(\phi, T) = \left(A + \frac{B}{T}\right) \cdot (c_1 + c_2 \cdot \phi + c_3 \cdot \phi^2) \quad \text{(Eqn. 7)}$$

where c_1, c_2 and c_3 are adjustable constants allowing to model the compositional dependence of χ.[54,59]

$$\chi(\phi) = c_1 + c_2 \cdot \phi \quad \text{(Eqn. 8)}$$

where c_1 and c_2 have the same meaning as the parameters used in Eqn. 7.

In contrast to other researchers, no "transformation of values to linearity" [46–48,54] was employed and the whole dataset was fitted with Eqns. 6-8 using the least-square fitting procedure, following the recommendation of Knopp and co-workers[61], who stated that: "From a statistical perspective, the potential of DSC measurements to make miscibility predictions

should be examined by deriving an objective function, which results in the unbiased, minimum variance properties of the least-square estimator." Table 3 presents the fitting parameters for the ITZ/EUD system as an example. Both datasets, determined from the onset and endset temperature values of the melting point were used. However, similar to the finding of Knopp et al.[61], the large standard deviations obtained for many of the adjustable parameters prevent an unambiguous description of the solid-liquid line beyond the points measured experimentally. Therefore, a part of the boundary between a fully isotropic and solid ITZ in Figure 8 in the range of ITZ concentrations 0-60% w/w is marked with a broken line marking uncertainty of the predictions.

Table 3. Fitting parameters for the solid-isotropic lines with standard deviation values as well as relative standard deviation values in parentheses. If the relative standard deviation is larger than 100%, it is expressed as >100%

Equation	Onset temperature values of ITZ melting event (RSD)	Endset temperature values of ITZ melting event (RSD)
Eqn. 6	A = -174±38 (22%) B = 74172±16263 (22%)	A = 685±164 (>100%) B = -301846±72488 (>100%)
Eqn. 7	A = -50±28246 (>100%) B = 23172±1.3·10^7 (>100%) c_1 = -3.7±2091 (>100%) c_2 = 12.5±7046 (>100%) c_3 = -11.6±6492 (>100%)	A = 129±547128 (>100%) B = -56955±2.41·10^8 (>100%) c_1 = 4.72±32056 (>100%) c_2 = 2.17±15668 (>100%) c_3 = -2.19±3605 (>100%)
Eqn. 8	c_1 = 4.50±1.23 (27%) c_2 = -9.63±1.92 (20%)	c_1 = 1.47±0.42 (29%) c_2 = -1.20±0.66 (55%)

3.4.4 Liquid crystalline phase separation

The phase diagrams for ITZ/polymers inclusive of LC phases are presented in Figure 8. Only onset temperature values were taken into considerations. The experimental enthalpy of the LC_{Sm-N} and LC_{N-I} transitions was taken to determine the boundary of the LC phase persistence shown by the broken lines parallel to the y-axis (Figure 8).

For the ITZ/EUD combination, the smectic phase was determined to be present for ITZ concentration above 60% w/w, while the nematic phase was persistent for ITZ contents above 85% w/w. The interaction parameter χ for the smectic-nematic and nematic-isotropic lines was determined to be 0.715±0.02 and 0.70±0.01, respectively, suggesting immiscibility of the LC phases with the polymer (Table 3). These values are close to that calculated for the solid-isotropic line, based on the endset points, which is 0.71±0.05 (Table 3). In contrast, the LC phases for the ITZ/HAS mixtures were still present at even around 50% w/w ITZ, however χ indicated, again, immiscibility of the API in a liquid crystalline state and the polymer (Table 3). The ITZ/CAR system only showed one LC phase, nematic, disappearing at ITZ concentrations below 80% w/w. The ITZ nematic phase was immiscible with CAR judging by the interaction parameter of 0.59±0.01 (Table 3).

The phase diagrams suggest that, depending on the polymer, the LC phase might be present even at a relatively large content of polymer in the binary combination, up to 50% w/w. The interaction parameters calculated for the smectic-nematic and nematic-isotropic lines were in line with those determined for the solid-isotropic lines based on the melting endset temperature values, implying immiscibility of LC ITZ and the polymer studied. Thus it can be concluded that in an ITR/polymer mix, if ITZ is present in an LC phase, immiscibility as a result of molecule anisotropy is expected.

3.4.3 Glass transition temperatures

If some of the API dissolves in the polymer matrix, then it will affect the T_g of the polymer.[15] T_g values were measured for the ITZ/polymer blends and are presented in Figure 8. The filled symbols represent compositions when all ITZ content is expected to be fully miscible with the polymer, while open symbols are T_g values of LC phase-separated systems. For miscible blends, the presence of a single T_g generally indicates that there is a single amorphous phase present. In contrast, the presence of more than one T_g would suggest that more than one

amorphous phase is present in the system. However, it needs to be kept in mind that blends showing only one T_g might be an indicator of miscibility achieved kinetically, due to intimate molecular mixing occurring in some of the processes.[62]

Single T_g values were measured for ITZ/EUD and ITZ/HAS at all compositions, however a deviation from linearity is evident for samples containing LC ITZ. For the ITZ/CAR dispersions, single T_g values were recorded at 90% and 95% of ITZ, however between 70% ITZ and 85% ITZ, two T_g values were shown on DSC thermograms. One of these T_g events appeared at a temperature of approximately 57 °C and most likely it corresponds to T_g of ITZ, while the temperature of the other T_g was seen to increase until it reached approximately 131 °C. The presence of two T_g events for ITZ/CAR systems imply a phase separation that is dependent on the API content. At and below 60% of ITZ, two T_g events were noticed, one that was of ITZ and the other of CAR. It was however clear from the phase diagrams (Figure 8) that no single T_g events should have been detected as at higher ITZ content the samples were phase separated due to the ITZ LC phase content.

Extrapolating (by linear fitting) the T_g values, for ITZ concentrations where no presence of LC phases was determined to 100% API content, the ITZ T_g values were found to be 46 and 33 °C, for ITZ/EUD and ITZ/HAS system, respectively. These values show some disparity, but are lower than that determined experimentally for the vitrified smectic phase of the drug and perhaps closer to the T_g of "amorphous" ITZ.

4. Conclusions

This work, for the first time, presents full phase diagrams for itraconazole/polymer systems showing a great abundance of phases, isotropic and anisotropic, that this dactive pharmaceutical ingredient, often used as a model drug substance to study amorphous polymeric solid dispersions, can form. With the phase identification sometimes misinterpreted, as evident

from the published literature, this work aimed to systematise the information on disordered itraconazole and show that binary mixtures of this substance with polymers not always are able to form fully disordered systems, however, depending on the itraconazole and polymer ratio, anisotropic, liquid crystalline and phase separated mixtures may form. The formation of such liquid crystalline blends is especially evident at high itraconazole to polymer content. The construction of thermodynamic phase diagrams, taking into consideration the presence of smectic and nematic phases, can be considered as a very beneficial guide in predicting the correct identity of the phases, of a key relevance to stability and formulation works.

5. Author information

Corresponding author

Dr. Lidia Tajber, School of Pharmacy and Pharmaceutical Sciences, Trinity College Dublin, Dublin 2, Ireland; lidia.tajber@tcd.ie, phone: 00353 1 896 2787.

Author contributions

The manuscript was written through contributions of all authors. All authors given approval to the final version of the manuscript.

Funding Sources

Synthesis and Solid State Pharmaceutical Centre (SSPC), financed by a research grant from Science Foundation Ireland (SFI) and co-funded under the European Regional Development Fund (Grant Number 12/RC/2275).

6. Acknowledgments

Research leading to these results was supported by the Synthesis and Solid State Pharmaceutical Centre (SSPC), financed by a research grant from Science Foundation Ireland

(SFI) and co-funded under the European Regional Development Fund (Grant Number 12/RC/2275).

Supporting Information

PXRD of physical mixtures after ball milling; PXRD of vitrified ITZ sample following heating to 163 °C; and determination of onset temperatures for the melting processes of ITZ/polymer mixtures. This material is available free of charge via the Internet at http://pubs.acs.org.

7. References

(1) Benet, L. Z. The Role of BCS (Biopharmaceutics Classification System) and BDDCS (Biopharmaceutics Drug Disposition Classification System) in Drug Development. *J. Pharm. Sci.* **2013**, *102* (1), 34–42.
(2) Patterson, J.; Bary, A.; Rades, T. Physical Stability and Solubility of the Thermotropic Mesophase of Fenoprofen Calcium as Pure Drug and in a Tablet Formulation. *Int. J. Pharm.* **2002**, *247* (1–2), 147–157.
(3) Hancock, B. C.; Parks, M. What Is the True Solubility Advantage for Amorphous Pharmaceuticals? *Pharm. Res.* **2000**, *17* (4), 397–404.
(4) Shalaev, E.; Wu, K.; Shamblin, S.; Krzyzaniak, J. F.; Descamps, M. Crystalline Mesophases: Structure, Mobility, and Pharmaceutical Properties. *Adv. Drug Deliv. Rev.* **2016**, *100*, 194–211.
(5) Demus, D., Goodby, J., Gray, G. W., Spiess, H.-W., Vill, V., Eds. *Handbook of Liquid Crystals*; Wiley-VCH Verlag GmbH: Weinheim, , 1998.
(6) Bunjes, H.; Rades, T. Thermotropic Liquid Crystalline Drugs. *J. Pharm. Pharmacol.* **2005**, *57* (7), 807–816.
(7) Yu, L. Amorphous Pharmaceutical Solids: Preparation, Characterization and Stabilization. *Adv. Drug Deliv. Rev.* **2001**, *48* (1), 27–42.
(8) Hilden, L. R.; Morris, K. R. Physics of Amorphous Solids. *J. Pharm. Sci.* **2004**, *93* (1), 3–12.
(9) Hancock, B. C.; Zografi, G. Characteristics and Significance of the Amorphous State in Pharmaceutical Systems. *J. Pharm. Sci.* **1997**, *86* (1), 1–12.
(10) Rades, T.; Padmadisastra, Y.; Müller-Goymann, C. C. Thermal Behaviour and Solubility of Fenoprofen Calcium. *Pharmazie* **1996**, *51* (11), 846–851.
(11) Serajuddln, A. T. M. Solid Dispersion of Poorly Water-Soluble Drugs: Early Promises, Subsequent Problems, and Recent Breakthroughs. *J. Pharm. Sci.* **1999**, *88* (10), 1058–1066.
(12) Marsac, P. J.; Shamblin, S. L.; Taylor, L. S. Theoretical and Practical Approaches for Prediction of Drug-Polymer Miscibility and Solubility. *Pharm. Res.* **2006**, *23* (10), 2417–2426.
(13) Caron, V.; Tajber, L.; Corrigan, O. I.; Healy, A. M. A Comparison of Spray Drying and Milling in the Production of Amorphous Dispersions of Sulfathiazole/Polyvinylpyrrolidone and Sulfadimidine/ Polyvinylpyrrolidone. *Mol.*

Pharm. **2011**, *8* (2), 532–542.
(14) Knopp, M. M.; Tajber, L.; Tian, Y.; Olesen, N. E.; Jones, D. S.; Kozyra, A.; Löbmann, K.; Paluch, K.; Brennan, C. M.; Holm, R.; Healy, A. M., Andrews, G. P., Rades, T. Comparative Study of Different Methods for the Prediction of Drug-Polymer Solubility. *Mol. Pharm.* **2015**, *12* (9), 3408–3419.
(15) Mucha, M. Polymer as an Important Component of Blends and Composites with Liquid Crystals. *Prog. Polym. Sci.* **2003**, *28* (5), 837–873.
(16) Peeters, J.; Neeskens, P.; Tollenaere, J. P.; Van Remoortere, P.; Brewster, M. E. Characterization of the Interaction of 2-Hydroxypropyl-β-Cyclodextrin With Itraconazole at PH 2, 4, and 7. *J. Pharm. Sci.* **2002**, *91* (6), 1414–1422.
(17) Dinunzio, J. C.; Miller, D. A.; Yang, W.; McGinity, J. W.; Williams, R. O. Amorphous Compositions Using Concentration Enhancing Polymers for Improved Bioavailability of Itraconazole. *Mol. Pharm.* **2008**, *5* (6), 968–980.
(18) Six, K.; Verreck, G.; Peeters, J.; Binnemans, K.; Berghmans, H.; Augustijns, P.; Kinget, R.; Van den Mooter, G. Investigation of Thermal Properties of Glassy Itraconazole: Identification of a Monotropic Mesophase. *Thermochim. Acta* **2001**, *376* (2), 175–181.
(19) Mugheirbi, N. A.; Paluch, K. J.; Tajber, L. Heat Induced Evaporative Antisolvent Nanoprecipitation (HIEAN) of Itraconazole. *Int. J. Pharm.* **2014**, *471* (1–2), 400–411.
(20) Six, K.; Leuner, C.; Dressman, J.; Verreck, G.; Peeters, J.; Blaton, N.; Augustijns, P.; Kinget, R.; Van den Mooter, G. Thermal Properties of Hot-Stage Extrudates of Itraconazole and Eudragit E100. Phase Separation and Polymorphism. *J. Therm. Anal. Calorim.* **2002**, *68* (2), 591–601.
(21) Janssens, S.; De Zeure, A.; Paudel, A.; Van Humbeeck, J.; Rombaut, P.; Van Den Mooter, G. Influence of Preparation Methods on Solid State Supersaturation of Amorphous Solid Dispersions: A Case Study with Itraconazole and Eudragit E100. *Pharm. Res.* **2010**, *27* (5), 775–785.
(22) Tarnacka, M.; Adrjanowicz, K.; Kaminska, E.; Kaminski, K.; Grzybowska, K.; Kolodziejczyk, K.; Wlodarczyk, P.; Hawelek, L.; Garbacz, G.; Kocot, A.; Paluch, M. Molecular Dynamics of Itraconazole at Ambient and High Pressure. *Phys. Chem. Chem. Phys.* **2013**, *15* (47), 20742–20752.
(23) Mapesa, E. U.; Tarnacka, M.; Kamińska, E.; Adrjanowicz, K.; Dulski, M.; Kossack, W.; Tress, M.; Kipnusu, W. K.; Kamiński, K.; Kremer, F. Molecular Dynamics of Itraconazole Confined in Thin Supported Layers. *RSC Adv.* **2014**, *4* (54), 28432–28438.
(24) Mugheirbi, N. A.; Fleischer, K.; Tajber, L. A Rare Case of Mesomorphic Behavior-Molecular Reorientation of Itraconazole Liquid Crystal Induced by a Hygrothermal Treatment. *Cryst. Growth Des.* **2016**, *16* (3), 1329–1336.
(25) Mesallati, H.; Umerska, A.; Paluch, K. J.; Tajber, L. Amorphous Polymeric Drug Salts as Ionic Solid Dispersion Forms of Ciprofloxacin. *Mol. Pharm.* **2017**, *14* (7), 2209–2223.
(26) Sarode, A. L.; Sandhu, H.; Shah, N.; Malick, W.; Zia, H. Hot Melt Extrusion (HME) for Amorphous Solid Dispersions: Predictive Tools for Processing and Impact of Drug-Polymer Interactions on Supersaturation. *Eur. J. Pharm. Sci.* **2013**, *48* (3), 371–384.
(27) Miller, D. A.; DiNunzio, J. C.; Yang, W.; McGinity, J. W.; Williams, R. O. Targeted Intestinal Delivery of Supersaturated Itraconazole for Improved Oral Absorption. *Pharm. Res.* **2008**, *25* (6), 1450–1459.
(28) Janssens, S.; de Armas, H. N.; Remon, J. P.; Van den Mooter, G. The Use of a New Hydrophilic Polymer, Kollicoat IR®, in the Formulation of Solid Dispersions of

Itraconazole. *Eur. J. Pharm. Sci.* **2007**, *30* (3–4), 288–294.
(29) Kaminska, E.; Tarnacka, M.; Kolodziejczyk, K.; Dulski, M.; Zakowiecki, D.; Hawelek, L.; Adrjanowicz, K.; Zych, M.; Garbacz, G.; Kaminski, K. Impact of Low Molecular Weight Excipient Octaacetylmaltose on the Liquid Crystalline Ordering and Molecular Dynamics in the Supercooled Liquid and Glassy State of Itraconazole. *Eur J Pharm Biopharm.* **2014,** *88* (3), 1094-104.
(30) Zhang, S.; Lee, T. W. Y.; Chow, A. H. L. Crystallization of Itraconazole Polymorphs from Melt. *Cryst. Growth Des.* **2016**, *16* (7), 3791–3801.
(31) Dwyer, L. M.; Michaelis, V. K.; O'Mahony, M.; Griffin, R. G.; Myerson, A. S. Confined Crystallization of Fenofibrate in Nanoporous Silica. *CrystEngComm* **2015**, *17* (41), 7922–7929.
(32) Sackmann, H. Thermodynamic Aspects of Polymorphism in Liquid Crystals. *Pure Appl. Chem.* **1974**, *38* (4), 505–527.
(33) Collings, P. J; Hird, M. *Introduction to Liquid Crystals: Chemistry and Physics*; CRC Press, Taylor and Francis Ltd.: London, 1997.
(34) Mugheirbi, N. A.; Tajber, L. Mesophase and Size Manipulation of Itraconazole Liquid Crystalline Nanoparticles Produced via Quasi Nanoemulsion Precipitation. *Eur. J. Pharm. Biopharm.* **2015**, *96*, 226–236.
(35) Fernandez-Ronco, M. P.; Salvalaglio, M.; Kluge, J.; Mazzotti, M. Study of the Preparation of Amorphous Itraconazole Formulations. *Cryst. Growth Des.* **2015**, *15* (6), 2686–2694.
(36) Piccinni, P.; Tian, Y.; McNaughton, A.; Fraser, J.; Brown, S.; Jones, D. S.; Li, S.; Andrews, G. P. Solubility Parameter-Based Screening Methods for Early-Stage Formulation Development of Itraconazole Amorphous Solid Dispersions. *J. Pharm. Pharmacol.* **2016**, *68* (5), 705–720.
(37) Rauch, S.; Selbmann, C.; Bault, P.; Sawade, H.; Heppke, G.; Morales-Saavedra, O.; Huang, M. Y. M.; Jákli, A. Glass Forming Banana-Shaped Compounds: Vitrified Liquid Crystal States. *Phys. Rev. E - Stat. Nonlinear, Soft Matter Phys.* **2004**, *69*, 021707.
(38) Donth, E.-J. *The Glass Transition; Relaxation Dynamics in Liquids and Disordered Materials*; Springer Series in Materials Science vol. 48; Springer: Berlin, 2001.
(39) Schmelzer, J. W. P.; Gutzow, I. S.; Mazurin, O. V.; Priven, A. I.; Todorova, S. V.; Petroff, B. P. *Glasses and the Glass Transition*; Wiley-VCH Verlag GmbH & Co. KGaA: Weinheim, Germany, 2011.
(40) Kerč, J.; Srčič, S. Thermal Analysis of Glassy Pharmaceuticals. *Thermochim. Acta* **1995**, *248*, 81–95.
(41) Rehage, G.; Frenzel, J. The Glass Transition and the Glassy State in Isotropic and Liquid Crystalline Polymers. *Br. Polym. J.* **1982**, *14* (4), 173–179.
(42) Dong, J.; Ozaki, Y.; Nakashima, K. Infrared, Raman, and near-Infrared Spectroscopic Evidence for the Coexistence of Various Hydrogen-Bond Forms in Poly(Acrylic Acid). *Macromolecules* **1997**, *30* (4), 1111–1117.
(43) Crawford, G. P.; Žumer, S. *Liquid Crystals in Complex Geometries*; CRC Press, Taylor and Francis Ltd.: London, 1996.
(44) Soulé, E. R.; Abukhdeir, N. M.; Rey, A. D. Thermodynamics, Transition Dynamics, and Texturing in Polymer-Dispersed Liquid Crystals with Mesogens Exhibiting a Direct Isotropic/Smectic-A Transition. *Macromolecules* **2009**, *42* (24), 9486–9497.
(45) Teraoka, I. *Polymer Solutions: An Introduction to Physical Properties*; John Wiley & Sons, Inc.: New York, 2002.
(46) Donnelly, C.; Tian, Y.; Potter, C.; Jones, D. S.; Andrews, G. P. Probing the Effects of Experimental Conditions on the Character of Drug-Polymer Phase Diagrams

Constructed Using Flory-Huggins Theory. *Pharm. Res.* **2015**, *32* (1), 167–179.
(47) Tian, Y.; Caron, V.; Jones, D. S.; Healy, A. M.; Andrews, G. P. Using Flory-Huggins Phase Diagrams as a Pre-Formulation Tool for the Production of Amorphous Solid Dispersions: A Comparison between Hot-Melt Extrusion and Spray Drying. *J. Pharm. Pharmacol.* **2014**, *66* (2), 256–274.
(48) Tian, Y.; Booth, J.; Meehan, E.; Jones, D. S.; Li, S.; Andrews, G. P. Construction of Drug-Polymer Thermodynamic Phase Diagrams Using Flory-Huggins Interaction Theory: Identifying the Relevance of Temperature and Drug Weight Fraction to Phase Separation within Solid Dispersions. *Mol. Pharm.* **2013**, *10* (1), 236–248.
(49) Marsac, P. J.; Li, T.; Taylor, L. S. Estimation of Drug-Polymer Miscibility and Solubility in Amorphous Solid Dispersions Using Experimentally Determined Interaction Parameters. *Pharm. Res.* **2009**, *26* (1), 139–151.
(50) Zhao, Y.; Inbar, P. Prediction of the Thermal Phase Diagram of Amorphous Solid Dispersions by Flory–Huggins Theory. *J. Pharm. Sci.* **2011**, *100* (8), 3196–3207.
(51) Bedjaoui-Alachaher, L.; Semdani, F.; Meziane, R.; Maschke, U. Thermophysical Analysis of Smectic a Domains Confined into a Thermoplastic Polymer Matrix. *Mol. Cryst. Liq. Cryst.* **2011**, *546*, 87–94.
(52) Srivastava, J. K.; Singh, R. K.; Dhar, R.; Singh, S. Phase Diagrams and Morphology of Polymer-Dispersed Liquid Crystals: An Analysis. *Liq. Cryst.* **2012**, *39* (11), 1402–1413.
(53) Benmouna, F.; Maschke, U.; Coqueret, X.; Benmouna, M. Mixtures of Polymer Networks and Nematic Liquid Crystals. *Mol. Cryst. Liq. Cryst. Sci. Technol. Sect. A. Mol. Cryst. Liq. Cryst.* **1999**, *330* (1), 475–482.
(54) Lin, D.; Huang, Y. A Thermal Analysis Method to Predict the Complete Phase Diagram of Drug-Polymer Solid Dispersions. *Int. J. Pharm.* **2010**, *399* (1–2), 109–115.
(55) Rubinstein, M.; Colby, R. M. *Polymer Physics*; Oxford University Press, 2006.
(56) Benmouna, R.; Benmouna, M. Thermophysical and Phase Properties of Polymer/Liquid Crystal Systems: Theoretical Aspects and Experimental Examples. *J. Chem. Eng. Data* **2010**, *55* (5), 1759–1767.
(57) Sun, Y. E.; Tao, J.; Zhang, G. G. Z.; Yu, L. Solubilities of Crystalline Drugs in Polymers : An Improved Analytical Method and Comparison of Solubilities of Indomethacin and Nifedipine in PVP , PVP / VA , and PVAc. *J. Pharm. Sci.* **2010**, *99* (9), 4023–4031.
(58) Forster, A.; Hempenstall, J.; Tucker, I.; Rades, T. Selection of Excipients for Melt Extrusion with Two Poorly Water-Soluble Drugs by Solubility Parameter Calculation and Thermal Analysis. *Int. J. Pharm.* **2001**, *226* (1–2), 147–161.
(59) Schuld, N.; Wolf, B. A. Solvent Quality as Reflected in Concentration- and Temperature-Dependent Flory-Huggins Interaction Parameters. *J. Polym. Sci. Part B Polym. Phys.* **2001**, *39* (6), 651–662.
(60) Kamide, K.; Sugamiya, K.; Kawai, T.; Miyazaki, Y. The Concentration Dependence of the Polymer–Solvent Interaction Parameter for Polystyrene–Methylcyclohexane System. *Polym. J.* **1980**, *12* (1), 67–69.
(61) Knopp, M. M.; Olesen, N. E.; Huang, Y.; Holm, R.; Rades, T. Statistical Analysis of a Method to Predict Drug-Polymer Miscibility. *J. Pharm. Sci.* **2016**, *105* (1), 362–367.
(62) Calahan, J. L.; Azali, S. C.; Munson, E. J.; Nagapudi, K. Investigation of Phase Mixing in Amorphous Solid Dispersions of AMG 517 in HPMC-AS Using DSC, Solid-State NMR, and Solution Calorimetry. *Mol. Pharm.* **2015**, *12* (11), 4115–4123.